Paper No.
19072

AMPP™
ANNUAL CONFERENCE + EXPO
MARCH 19-23, 2023 | DENVER, COLORADO

Impact of Fe_3O_4 on the Performance of an Imidazolinium-Based Inhibitor for Mitigation of CO_2 Corrosion of Carbon Steel

Maria Serenario, Bernardo Santos, Xi Wang, David Young, Marc Singer
Institute for Corrosion and Multiphase Technology
Department of Chemical and Biomolecular Engineering
Ohio University, Athens, OH 45701, USA

Maalek Mohamed-Said
TotalEnergies
OneTech - CSTJF, Avenue Larribau
F-64018 Pau, France

Alysson Helton Santos Bueno
CESTEq – Center of Surface Engineering, Tribology, and Electrochemistry
Department of Mechanical Engineering
Federal University of São João del Rei
170 Frei Orlando Square, São João del Rei, Brazil 36307352

ABSTRACT

Use of corrosion inhibitors to mitigate pipeline corrosion is common in the oil and gas industry. Despite this, few studies focus on how the presence of corrosion products affect their performance. This work aimed to understand the impact of Fe_3O_4 on the performance of a commercial primarily imidazolinium-based corrosion inhibitor formulation. A magnetite layer was formed in an autoclave at a high temperature (1 wt.% NaCl, N_2 sparged, pH 4, 120°C). The performance of the corrosion inhibitor was investigated with and without the presence of Fe_3O_4 (5 wt.% NaCl, CO_2, pH 4.5, 55°C). Linear polarization resistance (LPR) and potentiodynamic polarization were employed to study the effect of Fe_3O_4 on corrosion rate (CR) and inhibition efficiency (IE). Scanning electron microscopy (SEM) and Raman spectroscopy were used to characterize specimen surfaces. The acquired data showed that the presence of magnetite limited inhibitor performance. Dissolution of the magnetite layer over time in the CO_2 environment was also observed. This behavior was expected as the experiments were performed in non-thermodynamically favorable conditions for magnetite formation. Polarization sweeps indicated that the cathodic charge transfer and the limiting current of the H^+ reduction reaction were significantly accelerated due to the Fe_3O_4 layer. This behavior can be explained by the increase in cathodic reaction area due to the conductive nature of magnetite.

Keywords: Corrosion inhibition, Iron oxide, Magnetite, Inhibition efficiency, Potentiodynamic polarization

INTRODUCTION

Among the techniques disseminated in the industry to protect carbon steel pipelines against internal corrosion, the use of corrosion inhibitors (CIs) is one of the most common. Organic compounds containing nitrogen are commonly employed in the petroleum industry to decrease corrosion rates. The high inhibition efficiency can be attributed to adsorption capacity on the metallic surface, creating a protective film that interferes with the electrochemical reactions involved in the corrosion processes.[1–3]

The selection of appropriate corrosion inhibitors, however, poses several challenges. Typically, it is done through a lengthy and systematic testing process where the performances of each CI candidate are evaluated in simulated operating conditions. Yet, the corrosion inhibitor performances are commonly determined on carbon steel specimens with freshly polished surfaces – this is done to ensure consistency of the results but omits to consider the actual state of the pipeline internal surface. Under operating conditions, however, the internal pipeline surface is far from being neatly polished, and it may instead be covered by products of corrosion such as iron carbonate, sulfides, oxides (which form by precipitation) and/or carbide (which is the results of the dissolution of the ferrite phase). These layers can affect corrosion inhibition, and it is important to document their role. This study focuses on the role of magnetite in corrosion inhibition. Magnetite is not as commonly encountered in oil and gas production as carbonates or sulfides. However, magnetite can still be present on the steel surface in certain conditions: as a product of the manufacturing process (mill scale),[4,5] in cases of oxygen ingress[6] or at high-temperature applications (>120°C).[7,8] When investigating the influence of surface layers on corrosion inhibition, in this case, magnetite, several effects can be expected:

- Magnetite can act as a mass transfer barrier to species diffusing to and away from the metal surface, preventing CI from reaching the surface,
- Inhibitor molecules can adsorb preferentially on magnetite, decreasing the effective concentration of CI in bulk and limiting the CI efficiency, and possibly leading to surface heterogeneity and localized corrosion,
- Magnetite being a moderate electrical conductor, can create galvanic coupling with the surface and enhance the baseline corrosion rate, which in turn can decrease the CI efficiency,
- Since magnetite can be protective, a synergistic effect with CI is possible.

The research described herein focuses on the impact of the presence of Fe_3O_4 on the inhibition behavior in a simulated exploration production environment. A thick and uniform Fe_3O_4 layer was formed at high temperatures in an autoclave, thus providing a consistent method for magnetite formation. The inhibition behavior of an imidazolinium-based corrosion inhibitor was evaluated with and without the presence of Fe_3O_4 through linear polarization resistance (LPR) and potentiodynamic sweeps. Surface analysis techniques, including scanning electron microscopy (SEM), energy dispersive X-ray spectroscopy (EDS), and Raman spectroscopy, were employed to characterize the specimen surfaces after the magnetite formation and after the experiments at the exploration production environment.

EXPERIMENTAL PROCEDURE

Carbon steel specimens used for electrochemical measurements were machined from UNS G10180* carbon steel (C1018) with a ferritic-pearlitic microstructure with the specified elemental composition provided in Table 1. Before each experiment, the specimens were sequentially polished with 180, 400, and 600-grit silicon carbide abrasive papers, rinsed, and ultrasonically cleaned with isopropanol for two minutes. The specimens were then dried in nitrogen gas and stored in a desiccator.

* UNS numbers are listed in *Metals and Alloys in the Unified Numbering System*, published by the Society of Automotive Engineers (SAE International) and cosponsored by ASTM International.

Table 1
Composition (wt.%) of UNS G10180 carbon steel

Element	C	Mn	Si	Ni	Cu	Mo	S	Al	V	Ti	Nb	P	Fe
	0.16	0.65	0.25	0.055	0.088	0.019	0.01	0.007	0.002	0.001	0.002	0.009	balance

Experimental Method and Electrochemical Techniques

The experimental procedure consisted of a two-stage process (Figure 1). The first stage consisted of forming a magnetite layer on the surface of the specimen in a consistent and repeatable manner. To achieve this, the UNS G10180 carbon steel specimens were exposed to a high-temperature aqueous environment in an autoclave (Figure 2-a) to generate the magnetite layer. The specimens were characterized using Raman spectroscopy, scanning electron microscopy (SEM), and energy dispersive spectroscopy (EDS). The "magnetite" specimens (i.e., specimen covered with a magnetite layer) were stored under vacuum before being transferred to glass cells (Figure 2-b) and were tested both in the absence and presence of an imidazolinium-based commercial corrosion inhibitor, after which they were again characterized using the same techniques.

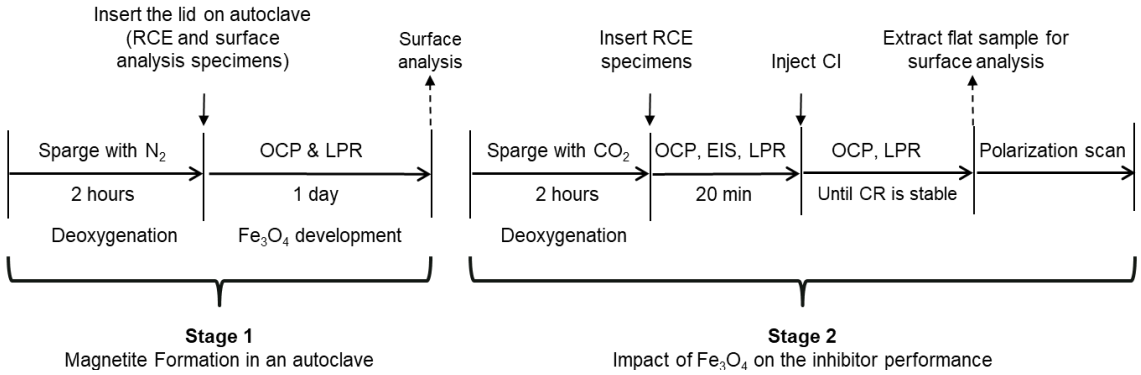

Figure 1: General experimental procedure.

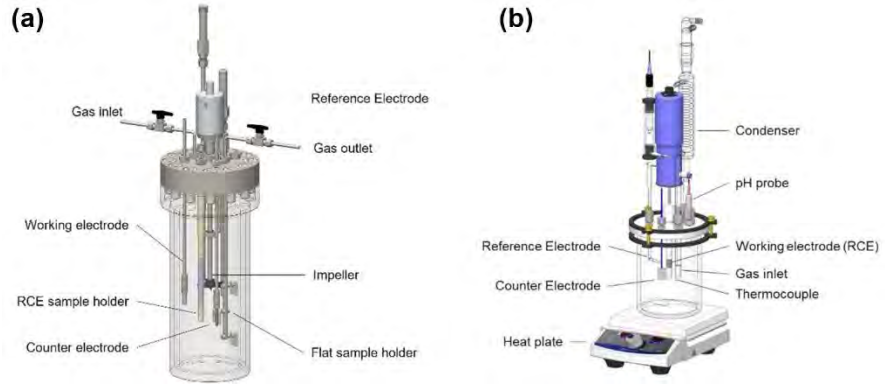

Figure 2: Experimental setup†. Note: (a) 4 L stainless steel autoclave setup used in Stage 1 in Figure 1; (b) 2 L glass cell setup used in Stage 2 in Figure 1.

The corrosion rate was assessed by linear polarization resistance (LPR) measurements, with a scan rate of 0.125 mV/s between ±5 mV vs. OCP, and B value of 26 mV.[9] Electrochemical impedance spectroscopy

† Image courtesy of Cody Shafer, ICMT, Ohio University.

(EIS) data were collected from 5kHz to 1 Hz with 7 points per decade with a perturbation amplitude of 5mV rms. Cathodic potentiodynamic polarization sweeps were conducted at the end of each experiment in the glass cell when the corrosion rates were stable. The anodic potentiodynamic sweeps were taken subsequently when the OCP returned to the original value; they were taken from the OCP up to +0.1 V vs. OCP. The ohmic drop was compensated for in all the presented curves. All electrochemical measurements were carried out via a potentiostat (Gamry Interface 1010‡).

Magnetite Formation

Carbon steel with a preformed Fe_3O_4 layer was generated following a methodology presented in the literature: the layers were performed in high-temperature condition and an N_2 environment.[8] This step was not done in a CO_2 environment in order to create a pure and uniform layer of Fe_3O_4 on the carbon steel surface and to avoid the formation of $FeCO_3$ (which is a standard corrosion product in the presence of CO_2). Magnetite was formed in a 4L stainless steel autoclave in a deaerated brine solution containing 1 wt.% NaCl in deionized water under anaerobic conditions at 120°C for 24 hours, as summarized in Table 2. A full schematic representation of the autoclave setup is shown in Figure 2-a. The autoclave was filled with 3000 mL of brine solution and purged with N_2 for at least 2 hours. Then the solution pH was adjusted at 80°C according to the water chemistry calculation to achieve pH 4.0 at 120°C. The magnetite formation experimental parameters are provided in Table 2.

Three geometries of UNS G10180 specimens were employed: 1) cylindrical specimens (rotation cylinder electrode, RCE, 1.4 cm in height and 1.2 cm in outer diameter) for inhibition experiments in the glass cell, 2) flat square specimens (1.0 cm x 1.0 cm x 0.2 cm) for weight loss and surface analysis, and 3) cylindrical specimen (2.0 cm in height and 1.0 cm in outer diameter) for electrochemical measurements in the autoclave. Once the specimens were in place, the autoclave was sealed and heated to 120°C. A three-electrode electrochemical cell setup was used: a high-temperature and high-pressure Ag/AgCl reference electrode, a Pt-coated Nb counter electrode, and the working electrode (UNS G10180 carbon steel, Table 1). OCP, EIS, and LPR measurements were performed to ensure that the surface conditions of the steel specimens were consistent among all sets of tests. The pH is monitored using a ZrO_2-based pH probe that can operate in high-temperature and high-pressure environments. A centrally located impeller was used to keep the solution fully mixed during each test. When the experiment was completed, the autoclave was depressurized. The specimens were then rinsed with deionized water and isopropanol and dried in air.

Table 2
Experimental matrix for magnetite formation

Description	Parameters
System	4 L stainless steel autoclave
Aqueous solution	1 wt.% NaCl
Material	UNS G10180
Sparge gas	N_2
Temperature	120°C
Initial pH	4.0 ± 0.1
Rotational speed of impeller	1000 rpm
Duration	1 day
Measurement Methods	OCP, LPR, weight loss
Surface Characterization	Raman spectroscopy, SEM/EDS

‡ Trade name

Inhibition Experiments

The magnetite specimens obtained from the autoclave experiments were immediately rinsed, dried, weighted, and stored in a desiccator before being inserted into a glass cell. The inhibition experiments were performed in a 2 L glass cell with a rotating cylinder electrode (Figure 2-b). All experiments were conducted at 55°C in the 5 wt.% NaCl solution saturated with CO_2 at pH 4.5, as summarized in Table 3. The conditions were selected based on a previous study by the authors.[10,11] and aimed at mimicking an environment typical of exploration & production. The solution was deoxygenated with CO_2 for at least 2 hours before each experiment. Sparging with CO_2 was maintained throughout the test to prevent O_2 ingress. A pH probe was inserted in the glass cell to monitor the pH changes. The electrolyte pH was adjusted throughout experiments to 4.5±0.1 with deoxygenated $NaHCO_3$ or HCl solutions, as necessary. After the insertion of the RCE specimen, the rotation speed was set at 1000 rpm. An imidazolinium-based commercial corrosion inhibitor package (50ppm_w) was injected into the solution directly using a syringe equipped with a long needle. The inhibitor concentration was above their bare steel surface saturation concentration, where the inhibited uniform corrosion rate would not decrease further if more corrosion inhibitor were added. It is important to mention that, at the time of this experimental series, no method had been developed to measure the CI concentration in the aqueous phase.

Table 3
Experimental matrix for the experiments in EP environment

Parameter	Condition
System	2 L glass cell with RCE
Aqueous solution	5 wt.% NaCl
Material	UNS G10180
Sparge gas	CO_2
Total pressure	1 bar
Temperature	55°C
pH	4.5 ± 0.1
Rotational speed of RCE	1000 rpm
Corrosion inhibitor	Imidazolinium-based (50 ppm_w)
Measurement Methods	OCP, LPR, potentiodynamic sweeps
Surface Characterization	Raman spectroscopy, SEM/EDS

A three-electrode electrochemical setup was used in this study, with a Pt-coated mesh as a counter electrode, a KCl saturated Ag/AgCl reference electrode connected to the glass cell via KCl salt bridge and a Luggin capillary, and C1018 RCE samples with and without the magnetite layer as a working electrode. For the uninhibited conditions, the OCP, EIS, and LPR were collected periodically for 5 hours until the LPR stabilized. The corrosion inhibitor was injected directly into the water phase for the inhibited conditions after a 20-minute pre-corrosion period. Subsequently, the OCP, EIS, and LPR were collected for 24 hours. The cathodic and anodic potentiodynamic polarization sweeps were collected at the end of the experiments. Each experiment was repeated twice.

RESULTS

Magnetite Formation

Corrosion rate

Electrochemical measurements were taken every 30 minutes over 24 hours in a deaerated N_2 environment at 120°C. These measurements facilitated real-time monitoring of the corrosion rate during

the magnetite formation. Figure 3 shows the LPR corrosion rates over time. The yellow circle series shows the corrosion rate calculated from the specimen weight loss at the end of each test. The weight measurement represents a value of general corrosion-averaged corrosion over the entire exposure time.

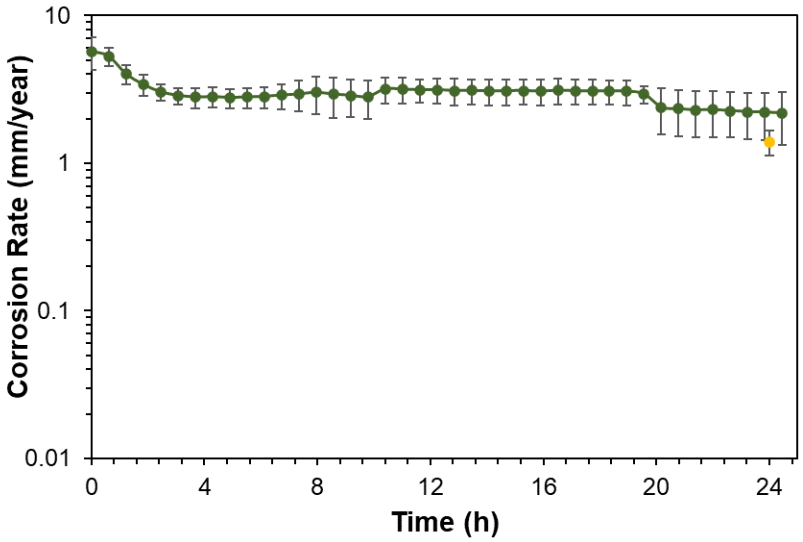

Figure 3: Corrosion rate over time in 1 wt.% NaCl at pH 4.0, 120°C, N_2.

For all experiments, the initial corrosion rates were around 5.6 mm/year. Then, the corrosion rates quickly decreased after 24 hours of the experiment and stabilized around 2.2 mm/year. The average LPR corrosion rate was comparable with the WL corrosion rate (yellow circle series) using a B value of 26 mV/decade.[9] It is important to note that in high-temperature tests, in addition to the Fe oxidation process, the measured current in the LPR also considers the oxidation of Fe^{2+} and Fe^{3+} ions in forming Fe_3O_4. The WL corrosion rate is more reliable and preferred in conditions with corrosion product formation since the surface kinetics could change with surface condition. In these conditions, the LPR corrosion rate only gives, at best, a trend, and caution should be taken in interpreting the data.

Surface analysis

The corrosion product layer on the steel surface was characterized by Raman spectroscopy. From Figure 4, the corrosion product was identified as magnetite (Fe_3O_4), where the characteristic magnetite peaks were identified, highlighting the strong peak at 670 cm^{-1} after 24 hours of experiment.[12,13]

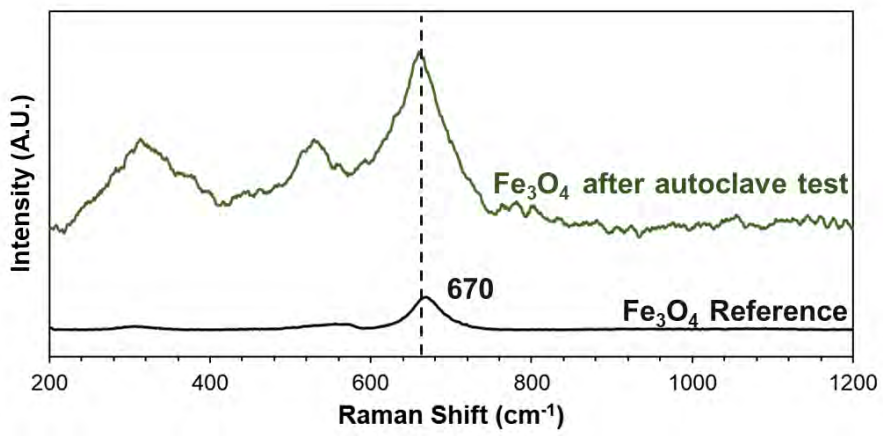

Figure 4: Raman spectra of magnetite samples.

The corrosion product morphologies and cross-section of steel specimens with a Fe_3O_4 layer after 24 hours in the 4L autoclave are shown in Figure 5 and Figure 6. The top view SEM images (Figure 5) showed the formation of a corrosion product layer, and the EDS results confirmed the presence of iron (Fe) and oxygen (O) on the surface, suggesting the presence of a Fe_3O_4 layer. A corrosion product layer is apparent from the cross-sectional view (Figure 6). After 24 hours of the experiment, a Fe_3O_4 layer (~7 µm) was formed. The EDS mapping scan also confirms that the layer was comprised of Fe and O, which means that the Fe_3O_4 became thick and compact rapidly. The fast formation of a Fe_3O_4 layer under a high-temperature environment has been confirmed in various studies.[8,14,15]

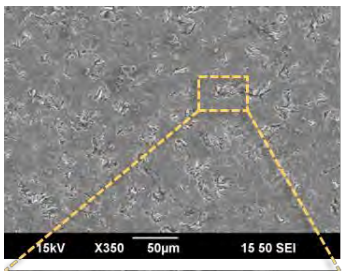

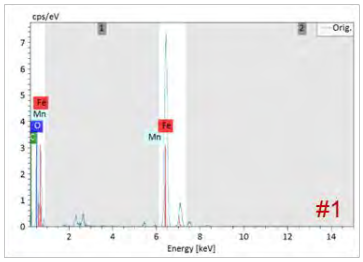

Element	At. No.	Mass [%]	Mass Norm. [%]	Atom [%]	abs. error [%] (3 sigma)
C	6	0.84	1.48	5.64	0.55
O	8	3.65	6.46	18.45	1.49
Mn	25	1.33	2.35	1.95	0.24
Fe	26	50.18	88.79	72.64	4.52
S	16	0.52	0.92	1.31	0.17
		56.52	100.00	100.00	

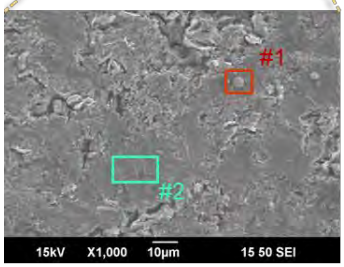

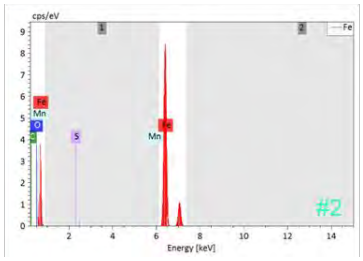

Element	At. No.	Mass [%]	Mass Norm. [%]	Atom [%]	abs. error [%] (3 sigma)
C	6	0.58	1.06	4.51	0.41
O	8	0.89	1.64	5.22	0.49
Mn	25	1.50	2.75	2.56	0.25
Fe	26	50.36	92.69	84.75	4.52
S	16	1.01	1.86	2.96	0.21
		54.33	100.00	100.00	

Figure 5: SEM images and EDS results after 24 hours of experiment, in 1 wt.% NaCl at pH 4.0, 120°C, N_2.

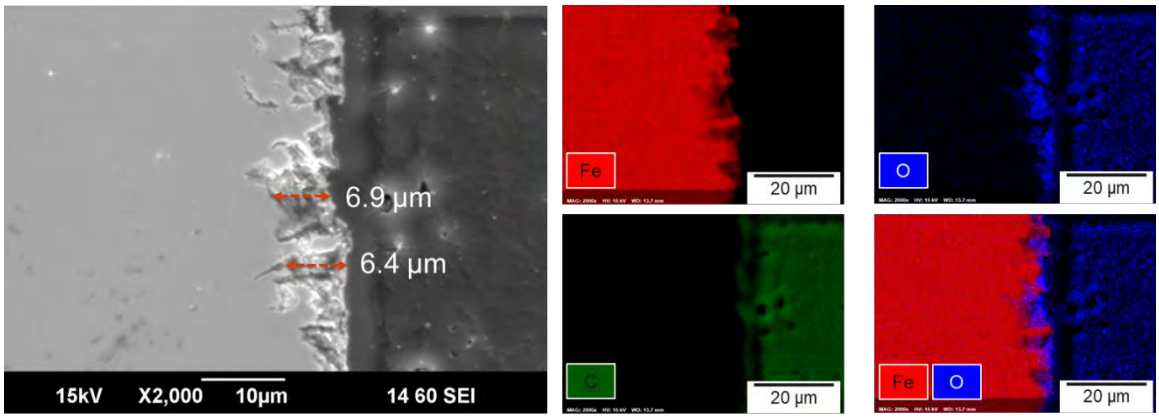

Figure 6: Cross-section and EDS mapping results for Fe, O, C distribution after 24 hours of experiment, in 1 wt.% NaCl at pH 4.0, 120°C, N_2.

These results show that a layer of magnetite did form on the metal surface but did not provide a significant level of protection against corrosion, indicating that the surface coverage was not total or that the layer retained a degree of porosity. The formed Fe_3O_4 film is partially consistent with the literature since some parameters of the experiments, such as the volume/surface ratio of the carbon steel exposed area, are not the same between the present work and the reference work, thus reducing precipitation of the Fe_3O_4 layer on the carbon steel surface.[8] Despite this, the setup adopted fulfills the requirement of the study, which is to form a magnetite layer on the steel surface.

Inhibition experiments

The effect of Fe_3O_4 on the inhibition of CI was examined in glass cell assays in the absence and presence of a primarily imidazolinium-based commercial corrosion inhibitor package (50 ppm_w). As previously reported, iron oxide (Fe_3O_4) was formed in the autoclave at a test temperature favorable to the precipitation of the iron oxide film (120°C). The experiments with glass cells were carried out at 55°C in 5 wt. % NaCl saturated with CO_2 at pH 4.5.

Corrosion rate

Figure 7 shows the corrosion rate evolution for uninhibited and inhibited (50 ppm_w of CI), with and without the Fe_3O_4 layer at 55°C.

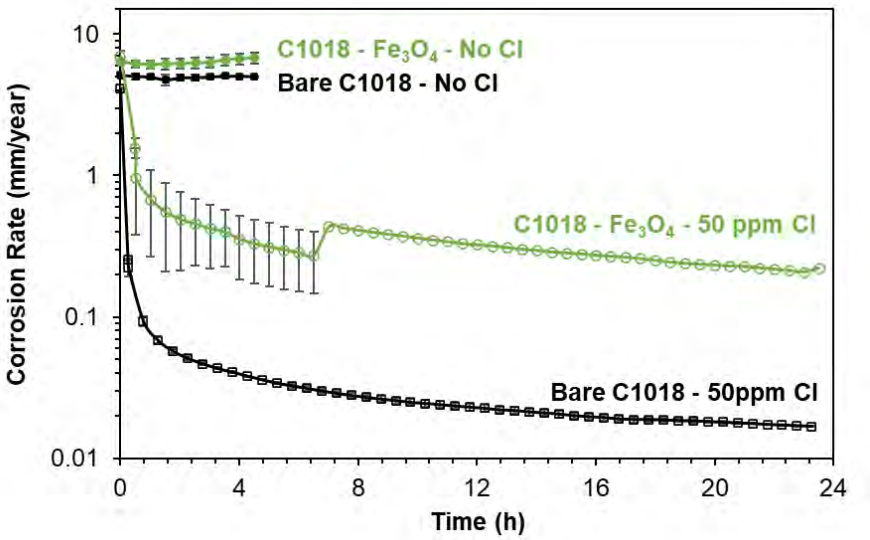

Figure 7. Corrosion rate over time in 5 wt.% NaCl at pH 4.5, 55°C, 0.86 bar CO_2.

For the uninhibited conditions, the corrosion rate of the specimens with and without Fe_3O_4 was stable and did not appreciably change after 5 hours, so the test was discontinuous. The specimen with the presence of the Fe_3O_4 layer, however, showed a higher corrosion rate than the bare steel specimen. This behavior can be explained by the semi-conductive nature of the Fe_3O_4, known to establish micro-galvanic cells with uncovered regions of the steel surface.[16,17] The micro-galvanic cells can also be formed between Fe_3C and the ferrite phase (α-Fe), resulting in the selective dissolution of the ferrite phase. The effect of cathodic regions of cementite is considerable in carbon steels with carbon content higher than approximately 0.15%.[18,19] In this work, the carbon steel used has a carbon content of 0.16%, as indicated in Table 1.

With the injection of 50 ppm_w of CI, the absolute values of the corrosion rate reduced significantly, stabilizing at 0.01 mm/year for the bare C1018 steel specimens and 0.22 mm/year for the C1018 specimens with the Fe_3O_4 layer. The reduction in corrosion inhibitor efficiency from 99.8% to 96.8% indicated that the presence of the Fe_3O_4 layer limited CI performance. Although magnetite is considered a protective film.[17] in tests where the film formation is not thermodynamically stable, the coexistence of film and inhibitor does not mean that the protection will be better; it will depend on the action of the inhibitor on the metal surface. Part of the film may remain on the steel surface, not promoting the protection and hindering the individual action of the inhibitor. The higher efficiency of the corrosion inhibitor on the bare steel surface, when compared to the specimen with the Fe_3O_4 layer, is not unexpected. The direct access of the inhibitor to the steel surface without the interference of the precipitated layer may favor the inhibitory action of the CI. In addition, the presence of a porous Fe_3O_4 layer can cause an increase in the surface area. Thus, the CI will act more efficiently in regions where the steel is directly exposed to the environment. However, confirming a positive synergistic effect between the Fe_3O_4 film and the CI was not possible at this stage.

Polarization Sweeps

Figure 8 compares the potentiodynamic polarization curves for carbon steel with and without the Fe_3O_4 layer obtained after 5 hours in uninhibited and 24 hours in inhibited conditions. The presence of the Fe_3O_4 layer led to an acceleration on the cathodic polarization curves. The increase in the limiting current density can be explained by the semi-conductive nature of Fe_3O_4, which acts as an additional cathodic area.

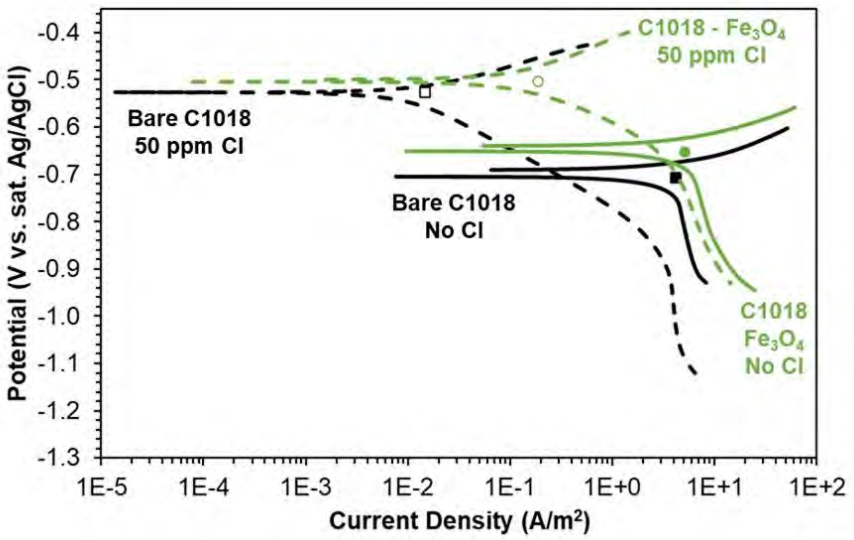

Figure 8. Potentiodynamic polarization curves in 5 wt.% NaCl at pH 4.5, 55°C, 0.86 bar CO_2

Under inhibited conditions, the anodic and cathodic polarization curves were retarded, while the limiting current density was unaffected for the condition without and with the Fe_3O_4 layer. However, the cathodic charge transfer region of the specimen with Fe_3O_4 (dashed light green lines) was accelerated compared with the same inhibited condition in the bare steel specimen (dashed black lines). This indicates that the CI adsorb on the steel surface (i.e., on the anodic ferrite phase) decreased the anodic dissolution rate as expected. However, the cathodic reaction rate (charge transfer and limiting current rates) was not reduced to the same level as the bare steel. It is hypothesized that this is due to an increase in the cathodic surface area associated with the presence of magnetite.

Surface Analysis

The galvanic coupling between the Fe_3O_4 and the carbon steel can explain the effect of the presence of magnetite. To further understand the inhibition of the CI on carbon steel with the presence of Fe_3O_4, it is essential to know how the corrosion product layer, Fe_3O_4, will behave in this environment.

Figure 9 shows the optical images of the C1018 specimens with the Fe_3O_4 layer before and after the inhibition experiments in the 2L glass cell. On the surface of the specimen, in the absence of CI, the Fe_3O_4 layer did not remain intact after 5 hours of the experiment. After 24 hours under inhibited conditions, the Fe_3O_4 layer exhibited significant dissolution over the entire surface of the specimen. The dissolution of Fe_3O_4 during the test reduced the thickness of the Fe_3O_4 layer in the specimens. Thus, no characteristic peak of the oxide was identified by Raman (Figure 10). The shear stress in the 2L glass cell does not reach values high enough to remove the corrosion products mechanically. Thus, the leading theory is that the degradation of magnetite was the effect of the chemical dissolution of the oxide layer.

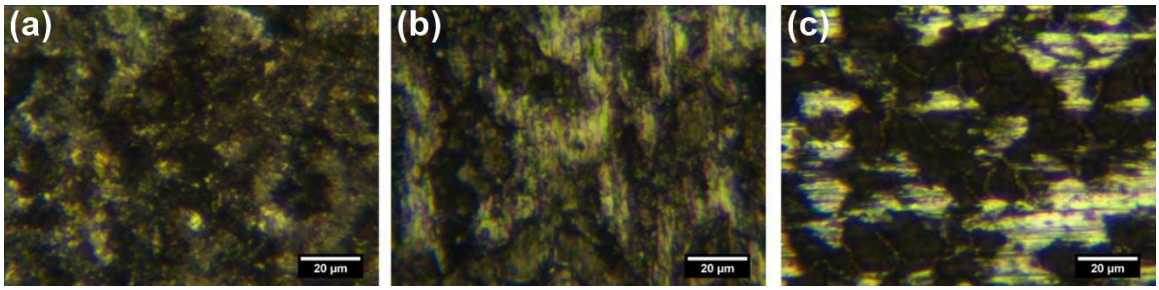

Figure 9. Optical images of specimens with the Fe_3O_4 layer before and after inhibition experiments in the 2L glass cell. Note: from the specimen with Fe_3O_4 layer after (a) autoclave test; (b) after 5 hours of the uninhibited experiment; (c) 24 hours of the inhibited experiment.

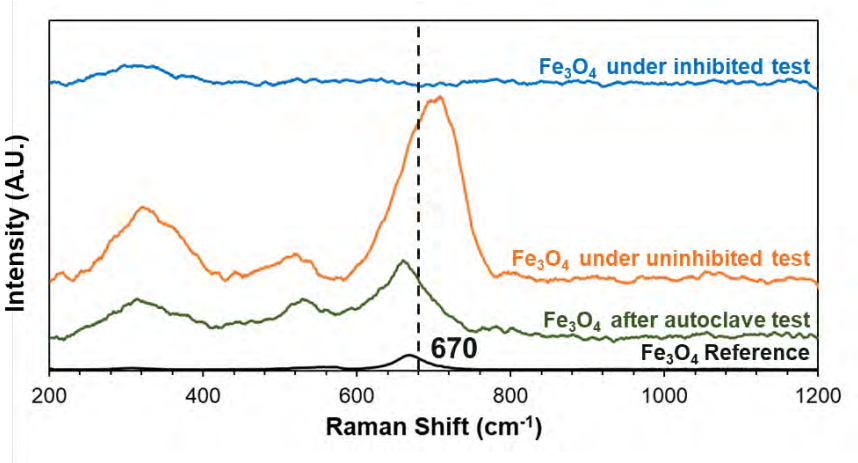

Figure 10. Raman spectra of C1018 specimens with the Fe_3O_4 layer before and after inhibition experiments in the 2L glass cell.

According to the literature, the magnetite layer, which can be protective, is rapidly dissolved or removed in turbulent flow.[17,20] Water chemistry characteristics, such as pH, dissolved oxygen, and temperature, affect the stability of the magnetite layer. When the magnetite layer is partially removed, the exposed metal surface of carbon steel is electrically connected with the remaining magnetite layer. The galvanic effect between the exposed metal surface of carbon steel and magnetite becomes more evident.[17,21]

Figure 11 shows SEM and EDS images of specimens layered with Fe_3O_4 before and after the inhibition experiments in the 2L glass cell. As already reported in the literature, the pH and temperature of the experimental conditions were not within the magnetite film stability region.[8,17] Thus, the dissolution of the layer was expected. However, the duration of the experiment was not long enough to observe the complete dissolution of the Fe_3O_4 layer in any of the test conditions. The sample under non-inhibited conditions showed further general corrosion along the entire surface (Figure 11-b). In the presence of Cl (Figure 11-c), a thinner layer of Fe_3O_4 layer than that observed in the formation of the layer in the autoclave (Figure 11-a) was observed, confirming that there was a process of dissolution of Fe_3O_4 in the tests carried out un the 2L glass cell. Despite the observed dissolution, no greater corrosive process of the substrate was noticed, indicating that the Fe_3O_4 dissolution was only partial. This result agreed with the corrosion rate trend and the optical images.

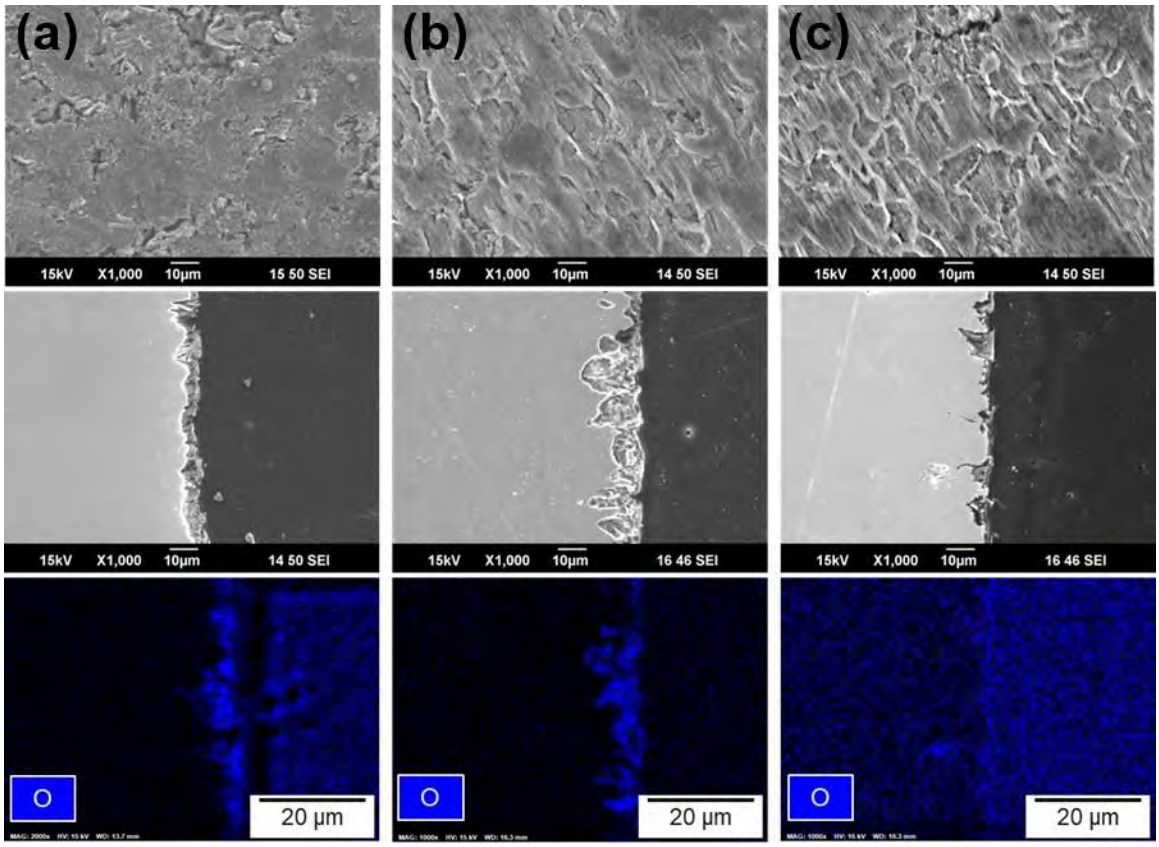

Figure 11: SEM images showing the morphologies, the cross-section view, and EDS mapping of C1018 specimens with the Fe_3O_4 layer before and after EP experiments in the 2L glass cell. Note: from the specimen with Fe_3O_4 layer after (a) autoclave test; (b) after 5 hours of the uninhibited experiment; (c) 24 hours of the inhibited experiment.

CONCLUSIONS

The formation of the Fe_3O_4 layer and the inhibition behavior of the imidazolinium-based corrosion inhibitor with and without the presence of Fe_3O_4 were evaluated. From this study, the following can be concluded:

- Fe_3O_4 could be formed consistently on the steel surface in a dedicated pre-treatment step. This step was performed in an N_2 environment and at a high temperature, favoring the formation of Fe_3O_4 while preventing the precipitation of any other products of corrosion. The Fe_3O_4 formed proved to be relatively porous and moderately protective.
- The presence of the Fe_3O_4 layer on the steel surface increased the bare steel corrosion rate in uninhibited CO_2 environments (circa 5-6 mm/year). This behavior could be attributed to the galvanic effect and increased cathodic surface area associated with a moderately conductive Fe_3O_4 layer.
- The presence of a commercial corrosion inhibitor reduced the corrosion rate values to approximately 0.01 mm/year in the absence of a Fe_3O_4 layer. This corrosion rate represented an inhibition efficiency of 99.8% concerning the condition without CI.
- In the presence of the Fe_3O_4 layer, adding CI promoted a reduction in corrosion rate values with values of 0.22 mm/year, reaching an inhibition efficiency of 96.8%. Despite the decrease in the corrosion rate, the presence of the Fe_3O_4 film reduced the efficiency of the commercial inhibitor.

- Surface analysis showed that the Fe_3O_4 layer formed in the autoclave underwent a partial dissolution when tested in pH 4.5 CO_2 saturated solution at 55°C, a condition in which Fe_3O_4 is not stable.
- Experiments at longer exposure time, with controlled CI bulk concentration, are required to assess further if efficiency as high as what has been seen on bare steel surfaces can be achieved given the complete dissolution of magnetite. The goal is to quantify CI molecules consumption by adsorption onto the porous magnetite layer, and consequently, CI depletion in the bulk aqueous phase.
- Experiments in the presence of a more dense and compact magnetite layer are required to further assess the effect of a very protective magnetite layer and if there is a positive synergy between the magnetite layer and corrosion inhibitor. Such tests will require CI test efficiency under conditions where the magnetite layer can be maintained, i.e., high temperature (>120°C).

ACKNOWLEDGEMENTS

This project has been supported by TotalEnergies. The authors would like to thank the financial support of TotalEnergies, CAPES (Coordenação de Aperfeiçoamento de Pessoal de Nível Superior – Brasil – Finance Code 001), CNPq (Brazilian National Council of Technological and Scientific Development - 405505/2021-3), and FAPEMIG (The Minas Gerais Research Funding Foundation – APQ-02540-21).

REFERENCES

1. M. Askari, M. Aliofkhazraei, A. Gha, A. Hajizadeh. “Film former corrosion inhibitors for oil and gas pipelines - A technical review”. Journal of Natural Gas Science and Engineering, 58 (2018), p. 92-114.
2. I. B. Obot, M. M. Solomon, S. A. Umoren, R. Suleiman, M. Elanany, N. M. Alanzi, A. A. Sorour. “Progress in the development of sour corrosion inhibitors: Past, present, and future perspectives”. Journal of Industrial and Engineering Chemistry, 79 (2019), p. 1-18.
3. I. B. Obot, I. B. Onyeachu, S. A. Umoren, M. A. Quraishi, A. A. Sorour, T. Chen, N. Ajeaban, Q. Wang. “High temperature sweet corrosion and inhibition in the oil and gas industry: Progress, challenges and future perspectives”. Journal of Petroleum Science and Engineering, 185 (2020), p. 106469.
4. J. Kargin, L. D. L. S. Valladares, L. E. Borja-Castro, J. Xize, D. G. Mukhambetov, Y. V. Jonyukhov, N. O. Moreno, A. G. Bustamante Dominguez, C. H. W. Barnes. “Characterization of iron oxide waste scales obtained by rolling mill steel industry”. Hyperfine Interactions, 243(2022), p. 11.
5. C. A. Barrero, A. L. Morales, M. L. Mejia, C. E.Arroyave. “On magnetite formation as a corrosion product of steel”. Hyperfine Interactions, (2002), p. 507-510.
6. N. R. Rosli, Y. S. Choi, D. Young. “Impact of oxygen ingress in CO_2 corrosion of mild steel”. NACE International Corrosion Conference, paper no. 4299 (San Antonio, TX: NACE, 2014), p. 15.
7. H. S. Gadiyar, N. S. D. Elayathu. “Corrosion and magnetite growth on carbon steels in water at 310°C – Effect of dissolved oxygen, pH, and EDTA addition”. Corrosion, 36(1980), p. 306-312.
8. S. Gao, B. Brown, D. Young, M. Singer. “Formation of iron oxide and iron sulfide at high temperature and their effects on corrosion”. Corrosion Science, 135(2018), p. 167-176.
9. S. Ren, Y. He, X. Wang, D. Young, M. Singer, M. Mohamed- Saïd. “The change of corrosion inhibition behavior of tetradecyl phosphate ester at elevated temperatures”. AMPP Annual Conference + Expo/2022, paper no.18053 (San Antonio, TX: AMPP, 2022), p. 12.
10. Y. He, S. Ren, X. Wang, D. Young, M. Singer, M. Mohamed-Said. “The effect of temperature on the adsorption behavior and inhibition performance of pyramidine-type inhibitor at medium temperature range (25°C to 80°C)”. AMPP Annual Conference + Expo/2022, paper no.17895 (San Antonio, TX: AMPP, 2022), p. 16.

11. S. Ren, Y. He, Z. Belarbi, X. Wang, D. Young, M. Singer. “Methodology for corrosion inhibitor characterization applied to phosphate ester and tetrahydropyrimidinium model compounds”. Corrosion Virtual Conference & Expo 2021, paper no. 16443, p. 17.
12. M. Hanesch. “Raman spectroscopy of iron oxides and (oxy)hydroxides at low laser power and possible applications in environmental magnetic studies”. Geophysics Journal International, 177 (2009), p. 941-948.
13. B. Lafuente, R. T. Downs, H. Yang, N. Stone. “The power of databases: The RUFF project”. From the book: Highlights in Minaralogical Crystallography, edited by T. Ambruster and R. M. Danisi, Gruyter (2016), p. 1-30.
14. T. Tanupabrungsun, D. Young, B. Brown, S. Nesic. “Construction and verification of Pourbaix diagrams for CO_2 corrosion of mild steel valid up to 250°C”. NACE Conference + Expo/2012, paper no.1418 (Houston, TX: NACE, 2012), p. 16.
15. S. Gao, B. Brown, D. Young, S. Nesic, M. Singer. “Formation mechanisms of iron oxide and iron sulfide at high temperature in aqueous H2S corrosion environment”. Journal of Electrochemistry Society, 165 (2018), p.C171-C179.
16. E. W. L. Chan. “Magnetite and its galvanic effect to the corrosion of carbon steel under carbon dioxide environments”. Thesis presented for the degree of Doctor of Philosophy of Curtin University, 2011.
17. G. D. Song, S. H. Jeon, Y. H. Son, J. G. Kim JG, D. H. Hur. “Galvanic effect of magnetite on the corrosion behavior of carbon steel in deaerated alkaline solutions under flowing conditions”. Corrosion Science, 131 (2018), p. 71-80.
18. M. Bonaventura, B. Brown, S. Ne, M. Singer. “Effect of flow and steel microstructure on the formation of iron carbonate”. Corrosion Journal. 75(2019), p. 1183-1193
19. D. A. López, W. H. Schereiner, S. R. Sánchez, S. N. Simison. “The influence of carbon steel microstructure on corrosion layers – An XPS and SEM characterization”. Applied Surface Science, 207(2003), p. 69-85.
20. V. Kain, S. Roychowdhury, P. Ahmedabadi, D. K. Barua. “Flow accelerated corrosion: Experience from contamination of components from nuclear power plants”. Engineering Failure Analysis, 18 (2011), p. 2028–2041
21. J. Owen, F. Ropital, G. R. Joshi, K. Kittel, R. Barker. “Galvanic interactions between surface layers and bare carbon steel in aqueous CO_2 environments”. AMPP Annual Conference + Expo/2022, paper no.17654 (San Antonio, TX: AMPP, 2022), p. 13.